

High-Resolution Time Profiles of Fiber Bursts at 1420 and 2695 MHz

P. Zlobec · M. Karlický

Received: 22 August 2013 / Accepted: 5 October 2013 / Published online: 13 November 2013
© Springer Science+Business Media Dordrecht 2013

Abstract To obtain constraints for models of fiber bursts, high-resolution time (0.01 s) profiles of the fiber bursts recorded at 1420 and 2695 MHz by the Trieste radiometers are studied in detail. The fiber bursts were identified using Ondřejov radio spectra. During the years 2000–2005, 18 intervals with fiber bursts were selected; 26 groups were defined and about 700 fibers were analyzed in detail. More than 300 pulsations, present almost simultaneously with the fibers, were also selected and studied in order to find similarities or differences between these two types of fine structures. It was found that the polarization of the associated continuum, both for fiber bursts and pulsations, is practically the same. Evaluating the ratio between absorption over emission of many single fibers we found that this parameter is very different even for nearby bursts; however, we realized that this ratio shows a tendency to decrease with time. Finally, the time profile of one selected fiber burst was fitted using a recent model based on the modulation of the broadband radio emission by fast magnetoacoustic waves. The results are discussed.

Keywords Sun: flares · Sun: radio radiation · Methods: data analysis

1. Introduction

Fiber bursts (fibers) are particular fine structures that are observed in some type IV radio events. They can be present in a rather large frequency band and show an intermediate frequency drift when compared to those of type II and type III radio bursts. In single frequency records, a typical fiber shows an initial absorption phase (with respect to the continuum) followed by an emission one.

P. Zlobec
INAF – Trieste Astronomical Observatory, Via G.B. Tiepolo 11, 34143 Trieste, Italy
e-mail: zlobec@oats.inaf.it

M. Karlický (✉)
Astronomical Institute, Academy of Sciences of the Czech Republic, 251 65 Ondřejov, Czech Republic
e-mail: karlicky@asu.cas.cz

Generally, fibers are present at frequencies below 1 GHz, or, in fact, their existence at frequencies below this value are assumed in the older works; see Young *et al.* (1961), Chernov (1976), Slottje (1981), Elgaroy (1982), and Bernold and Treumann (1983). However, fibers can be observed also at frequencies higher than 1 GHz. Benz and Mann (1998) studied such bursts in the range 1–3 GHz, and Wang and Zhong (2006) detected them at 2.6–3.8 GHz. For an overview of these bursts, see Chernov (2011).

Slottje (1981) used Utrecht spectrographic data (observations up to 950 MHz) and derived some statistical parameters pertinent to fibers. In particular, he noted that the polarization of the continuum and of the superimposed fibers is practically the same. In Table 2 (Chapter 5.3.2.1) of his booklet, he showed that, of the 3911 fibers he analyzed, the ones with both absorption and emission phases were the most common (90 %), the ones with only an emission phase were rather rare (1.5 %), while those with only an absorption phase were the rarest (0.5 %); other cases were unclear. The number of fibers he considered at around 180, 240, and 300 MHz (each frequency range was 40 MHz wide) were 201, 631, and 3000, respectively. The duration at a single frequency was typically 0.2–0.4 s in the whole range (150–900 MHz).

There are two types of fiber models, those based on: a) whistler waves (Kuijpers, 1975; Mann, 1990; Mann, Karlický, and Motschmann, 1987) and b) Alfvén waves or solitons (Treumann, Güdel, and Benz, 1990). These models are used for the estimation of the coronal magnetic fields (Benz and Mann, 1998; Rausche *et al.*, 2007). Thus, the theory and interpretation of fibers are relevant to the determination of the physical parameters of the perturbed low layers of the solar corona. Furthermore, Kuznetsov (2006) proposed a model based on the modulation of the radio continuum by magnetohydrodynamic waves. Recently, Karlický, Mészárosová, and Jelínek (2013) have shown that some fibers are connected with fast sausage magnetoacoustic wave trains. Based on this fact, they have developed a semi-empirical model (similar to that of Kuznetsov (2006)), and also a full magnetohydrodynamic model of fibers.

We are not aware of articles dealing with detailed measurements of fiber profiles recorded at single frequencies, especially regarding their emission and absorption phases. Therefore, in the present article we study these particular characteristics using high time resolution records. The polarization characteristics is another topic of our interest. We think that this detailed study sets constraints for present models of fiber bursts. We also fit a typical fiber profile using the recently developed fiber model (Karlický, Mészárosová, and Jelínek, 2013) and determine the density parameters of the corresponding magnetoacoustic wave.

2. Data

In Table 1 we present the considered intervals with fibers at 1420 MHz; the last interval was recorded at 2695 MHz. Related X-ray flares are also given.

We realize that the presence of fibers is related to rather strong (importance C, M, and X) and long lasting flares. Fibers are mostly present in the late phase of the flare evolution, however, they can also appear near their maximum or more rarely near their start time. Fibers are generally superposed on rather strong continua. The sense of the polarization of fibers shows no hemispheric preference pattern. Highly polarized events originate from sources that are disposed not far from the solar disk center (*i.e.* up to 52° E or W).

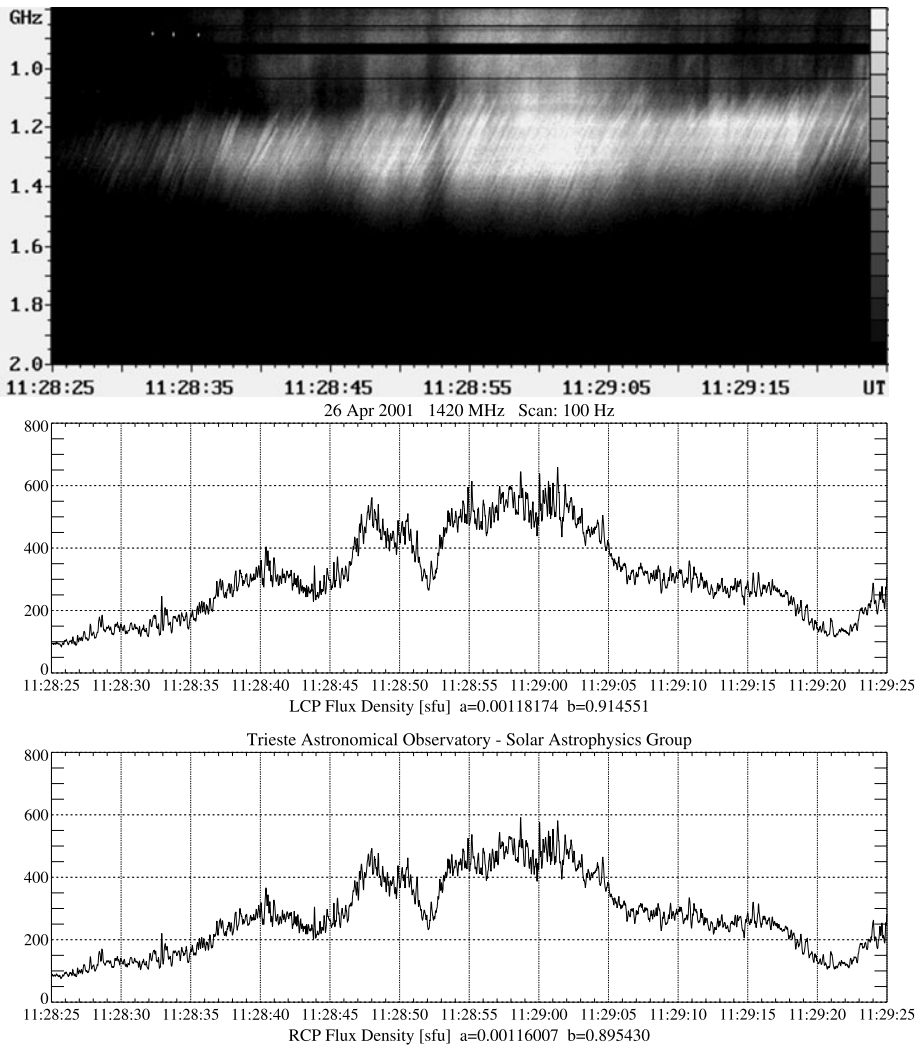
An example of a group of fibers recorded by the Ondřejov radiospectrograph and the Trieste radiopolarimeter is shown in Figure 1.

Table 1 Time intervals when fibers were present and related X-ray flares. The fibers were observed at 1420 MHz, the only exception is the interval in the last line when fibers were observed at 2695 MHz.

Event	Radio		GOES			
	Start [UT]	End [UT]	Start [UT]	Max [UT]	End [UT]	X-ray Imp.
14 July 2000	10:42:58	10:43:42	10:03	10:24	10:43	X5.7
14 July 2000	10:48:50	10:49:56	10:03	10:24	10:43	X5.7
14 December 2000	09:50:10	09:50:23	09:34	09:58	11:00	C3.4
15 April 2001	14:33:04	14:34:25	13:19	13:50	13:55	X14.4
26 April 2001	11:26:05	11:31:10	11:26	13:12	13:19	M7.8
26 April 2001	11:41:50	11:42:58	11:26	13:12	13:19	M7.8
19 July 2001	10:01:50	10:06:35	09:52	10:04	10:17	M1.8
19 July 2001	10:27:35	10:29:05	09:52	10:04	10:17	M1.8
19 July 2001	10:33:50	10:39:00	09:52	10:04	10:17	M1.8
16 September 2001	07:42:30	07:43:00	07:39	07:45	07:51	C4.5
17 September 2001	08:22:00	08:23:00	08:18	08:25	08:34	M1.5
20 September 2001	14:38:15	14:39:05	14:35	14:41	14:45	C3.4
09 October 2001	10:58:30	11:10:00	10:46	11:13	11:49	M1.4
22 November 2001	09:50:10	09:50:42	08:01	08:39	08:51	C1.3
07 April 2002	14:19:33	14:20:55	14:17	14:29	14:42	C2.8
18 November 2003	08:33:40	08:41:40	08:12	08:31	08:59	M3.9
11 July 2005	16:34:00	16:40:19	14:56	15:08	15:23	C8.4
15 April 2001	14:23:01	14:24:30	13:19	13:50	13:55	X14.4

We were looking for observations where fibers were evident both in radio spectra (Ondřejov Observatory) and in polarimetric single frequency records (National Institute for Astrophysics (INAF) Trieste Astronomical Observatory). The Ondřejov radio spectra cover the range 0.8–2 GHz and 2–4.5 GHz with time resolution 0.1 s (Jiříčka *et al.*, 1993). The Trieste single frequency data are recorded in the polarimetric right (R) and left (L) channels at 1420 and at 2695 MHz with a time resolution of 0.01 s. We use observations at 1420 MHz (13 days/17 intervals) and at 2695 MHz (one day/one interval). Generally fibers appear in groups; different groups or very long lasting groups form intervals.

The selection of fibers was made with care, considering the events that appear in both types of records. Our aim was the selection of relatively strong, prominent events showing (in single frequency record) smooth profile (*i.e.* not complex events); only exceptionally some complex events were selected. The smooth profile is evident during the emission phase, while the (generally weaker) absorption phase may be disturbed due to the presence of low-intensity bursts superimposed on the continuum. Due to the same problem, the true level of the continuum is also difficult to determine (*i.e.* it is questionable). It is also obvious that when fibers appear very close in time, the absorption part could be distorted by the emission phase of the previous burst; such cases were not considered. We are convinced that a high number of events on different days and within different intervals is important for an analysis of their characteristics.



IDL environment programmed by S. Padovan

Figure 1 Example of the radio spectrum with fiber bursts recorded during the flare on 26 April 2001 (interval 11:28:25–11:29:25 UT) in the range 800–2000 MHz by the Ondřejov radiospectrograph (upper panel) together with the 1420 MHz L- and R-polarized radio-flux profiles by the Trieste radiopolarimeter (middle and bottom panels, respectively).

3. Description of Fiber Events and Results

In radio spectra, a group of individual fibers show different drifts (generally negative). We analyzed them at 1420 MHz and determined drift values in the range -45 – (-110) MHz s^{-1} ; for one group at 2695 MHz the average drift results to be about -300 MHz s^{-1} .

We found that each group of fibers, present in the time intervals reported in Table 1, shows its own characteristics, so that it is not possible to generalize them. That holds both for the spectral aspect and for the single frequency records.

We confirm the result reported by Slottje (1981) that the polarization of fibers is very similar to the value pertinent to the continuum (measured at 1420 or at 2695 MHz) on which the fibers are superposed and originate from; the same is valid also for large bandwidth pulsations that are present in 55 % of the considered time intervals.

We selected numerous such (possibly “nice”) examples for both types of fine structures. We measured their characteristic parameters at 1420 and 2695 MHz in order to find differences or similarities between them. In particular, for each selected burst we evaluated the intensity (*i.e.* minimum to maximum emission range), using sfu units, separately in the left (L) and right (R) polarimetric component, the duration at half power, the polarization and the delay between the L and R components during the increasing and the decreasing phases (see columns 4 and 5 in Table 2). The delay measurements are dealing with small values (few ms) and are rather delicate (in particular this delay cannot be measured when the component of one polarimetric channel is weak (*i.e.* in strongly polarized events)). Remarkable delay mean values are given only in the first two lines of Table 2 (data for 14 July 2000). This table reports mean data pertinent only to fibers. Polarization and delay between the L and R components show nearly the same values for fibers and pulsations. That should mean that continuum, fibers, and pulsations that are emitted at the same time should come from the same source or from a nearby region having very similar physical characteristics.

For each selected fiber we evaluated its part in absorption and in emission, *i.e.* I_a/I_e gives the ratio of the intensity in absorption and in emission; d_e is the duration (at half power) of the emission part, and, analogously, d_a gives the duration of the part in absorption. The product $I_e \cdot d_e$ represents a rough value of the emitted “energy” above the continuum, meanwhile $I_a \cdot d_a$ gives the same for the absorption part. We also determined the ratio of these “energies” ($I_a \cdot d_a$)/($I_e \cdot d_e$). Generally I_a/I_e and ($I_a \cdot d_a$)/($I_e \cdot d_e$) are lower than one, the cases when the value is zero are rather common, the absence of I_e is very rare. Mean values are reported in Table 3.

Let us note that the ratio I_a/I_e (and ($I_a \cdot d_a$)/($I_e \cdot d_e$)) is generally different for each selected event in a group of fibers (the only exception holds when in a group the absorption is absent) and therefore the spread is very large, as it is similar to the main value itself. Mean values of I_a/I_e are similar to the ones of ($I_a \cdot d_a$)/($I_e \cdot d_e$); only in one example (26 April 2001) they are substantially different but the spread of ($I_a \cdot d_a$)/($I_e \cdot d_e$) is abnormally large.

The mean duration of fibers belonging to different groups represents a quite large interval of values (range 56–525 ms) (see Tables 2 and 3), which probably indicates different physical conditions where they are coming from; while in general the mean duration of pulsations is more limited in spread (range 40–64 ms).

We realized that there is no relationship between the duration of fibers and the duration of pulsations that are present at nearly the same time.

In the following sections we briefly describe the characteristics of fibers and the related structures that are present in the selected groups at 1420 and 2695 MHz. Particular remarks that are typical for each considered group are also given.

3.1. 14 July 2000 Event at 1420 MHz, Interval 10:42:58–10:43:42 UT

The spectrum shows a mixture of large frequency pulsations (< 1000 MHz–1550 MHz) and fibers (< 1000–1450 MHz). Pulsations (about 5 per second) are generally weaker than the fibers (randomly present). For each of the selected bursts we evaluated the parameters as mentioned above; the mean values for fibers are given in Table 2. The mean delay values between the polarimetric components L and R are similar for fibers and pulsations (about –7 ms), the delay is practically the same during the increasing and the decreasing part of

Table 2 Mean values of parameters for each group of fibers considered as bursts. The interval reports the time of the first and of the last selected fiber and Nr represents their number. Delays up (down) report delays between the L and R polarised components during the increasing (decreasing) part of the burst. The fibers were recorded at 1420 MHz; the only exception is the last event (at 2695 MHz).

Event interval (UT)	Nr	Duration (ms)	Delay up (ms)	Delay down (ms)	Polarization (%)
14 July 2000 10:43:09 – 10:43:37	11	82.7 ± 25.3	-5.3 ± 2.6	-8.9 ± 4.3	66.3 ± 4.9 R
14 July 2000 10:49:06 – 10:49:56	24	113.1 ± 39.6	-16.1 ± 5.1	-17.9 ± 6.6	69.8 ± 8.6 R
14 December 2000 9:50:13 – 9:50:19	5	92.0 ± 21.8			90.6 ± 1.9 R
15 April 2001 14:33:08 – 14:33:33	8	139.3 ± 59.0	~ 0	~ 0	13.8 ± 8.8 L
26 April 2001 11:26:11 – 11:26:28	11	91.6 ± 24.8	~ 0	~ 0	10.3 ± 6.9 L
26 April 2001 11:26:52 – 11:28:08	56	107.8 ± 38.7	~ 0	~ 0	6.4 ± 5.9 L
26 April 2001 11:28:28 – 11:29:19	59	106.3 ± 38.2	~ 0	~ 0	5.3 ± 4.0 L
26 April 2001 11:29:21 – 11:31:05	101	109.1 ± 48.3	~ 0	~ 0	5.3 ± 3.3 L
26 April 2001 11:42:20 – 11:42:52	28	112.4 ± 49.5	~ 0	~ 0	26.0 ± 5.5 L
19 July 2001 10:04:16 – 10:05:15	36	77.8 ± 21.6	-0.2 ± 2.1	1.0 ± 3.3	12.0 ± 4.6 L
19 July 2001 10:05:30 – 10:06:29	19	73.1 ± 11.6	-0.6 ± 3.6	0.3 ± 2.8	12.2 ± 2.4 L
19 July 2001 10:35:07 – 10:36:07	39	87.2 ± 29.4	-1.2 ± 1.2	-1.5 ± 1.7	20.1 ± 5.4 L
19 July 2001 10:38:49 – 10:38:59	13	61.5 ± 27.2	-0.6 ± 1.2	-0.4 ± 1.6	10.1 ± 3.0 L
16 September 2001 7:42:31 – 7:42:35	5	163.7 ± 18.8	~ 0	~ 0	1.4 ± 3.8 L
17 September 2001 8:22:22 – 8:22:52	49	37.3 ± 5.4			85.2 ± 10.0 R
20 September 2001 14:38:42 – 14:38:58	19	62.0 ± 22.5	1.1 ± 2.2	1.6 ± 2.4	34.8 ± 4.2 L
9 October 2001 11:00:48 – 11:01:45	9	225.6 ± 117.0			5.7 ± 2.9 L
22 November 2001 09:50:37 – 09:50:37	1	524.5			94 R
7 April 2002 14:19:42 – 14:19:44	8	94.50 ± 27.3	-0.8 ± 1.0	-0.8 ± 2.8	21.5 ± 5.4 L
18 November 2003 8:35:00 – 8:36:00	26	102.8 ± 24.7			92.5 ± 1.8 R
18 November 2003 8:36:12 – 8:37:48	25	124.2 ± 32.8			93.7 ± 2.3 R
18 November 2003 8:38:01 – 8:41:40	21	95.5 ± 19.6			95.0 ± 3.2 R

Table 2 (Continued.)

Event interval (UT)	Nr	Duration (ms)	Delay up (ms)	Delay down (ms)	Polarization (%)
11 July 2005 16:34:22 – 16:36:17	35	62.5 ± 17.9			92.6 ± 1.4 R
11 July 2005 16:36:22 – 16:36:59	11	55.7 ± 14.0			92.7 ± 2.0 R
11 July 2005 16:37:11 – 16:40:18	30	77.9 ± 28.0			93.0 ± 1.9 R
15 April 2001 14:23:03 – 14:23:51	45	83.6 ± 43.6	~ 0	~ 0	12.4 ± 3.1 R

the bursts. The negative delay means that the left (L) (*i.e.* weaker) component of the burst is delayed in respect to the right (R) component of the same burst. Such result is not unique as another polarized fiber (recorded at 237 MHz) with delay (20 ms) of the weakest component (L) was reported in Chernov and Zlobec (1995). The time delay of the components were also found in narrowband spikes (2–8 ms) (Zlobec and Karlický, 1998) and in pulsations (up to 20 ms) (Fleishman *et al.*, 2002). The mean duration of fibers and of pulsations is different: about 83 and 43 ms, respectively. Fibers generally show a complex structure.

3.2. 14 July 2000 Event at 1420 MHz, Interval 10:48:50 – 10:49:56 UT

Large frequency pulsations (< 1000–1500 MHz) are present at the beginning of this interval, fibers (< 1000–1650 MHz) are more common and prominent afterwards. In the single frequency records the fibers generally show rather complex structure. Pulsations (about 12 per second) are generally weaker than fibers. The mean delay between the two polarimetric components is similar (–17 ms) for fibers and pulsations.

3.3. 14 December 2000 Event at 1420 MHz, Interval 9:50:10 – 9:50:23 UT

The spectrum shows a mixture of large frequency pulsations (< 1000 MHz–1700 MHz) and fibers (1000–1600 MHz). Fibers have no absorption phase or it is very underdeveloped, so the ratios I_a/I_e and $(I_a \cdot d_a)/(I_e \cdot d_e)$ are about zero. We selected only a few fibers as in this interval they are not prominent.

3.4. 15 April 2001 Event at 2695 MHz, Interval 14:23:01 – 14:24:30 UT

The continuum at 2695 MHz starts to grow at 14:20:30 UT; the structure is complex. The strongest and longest enhancement is developing between 14:23:03 and 14:23:50 UT when a nice group of fibers is present. In the spectrum fibers are present up to 3 GHz; no other fine structures are evident. In the single frequency records the fibers generally show a rather complex structure. The emission and the absorption phases of the selected fibers are very different, as happens for the fibers at 1420 MHz.

3.5. 15 April 2001 Event at 1420 MHz, Interval 14:33:04 – 14:34:25 UT

The fibers occupy the frequency interval 1200–1450 MHz. The selected ones are present in the very early part of the interval, when it is possible to distinguish them from the strongest pulsations (range 1000–2000 MHz).

Table 3 Mean values of I_a/I_e , $(I_a \cdot d_a)/(I_e \cdot d_e)$, duration during emission d_e and absorption d_a and range of intensity for fibers in the groups quoted in Table 2.

Event	I_a/I_e	d_e (ms)	d_a (ms)	$(I_a \cdot d_a)/$ $(I_e \cdot d_e)$	Intensity (sfu)
14 July 2000 10:43:09 – 10:43:37	0.32 ± 0.19	66.5 ± 20.5	74.8 ± 40.1	0.34 ± 0.27	170 – 1000
14 July 2000 10:49:06 – 10:49:56	0.40 ± 0.29	83.9 ± 32.1	73.3 ± 43.4	0.43 ± 0.45	50 – 580
14 December 2000 9:50:13 – 9:50:19	~ 0	92.0 ± 21.8	~ 0	~ 0	90 – 200
15 April 2001 14:33:08 – 14:33:33	0.32 ± 0.16	96.6 ± 28.9	130.5 ± 85.6	0.54 ± 0.45	80 – 130
26 April 2001 11:26:11 – 11:26:28	0.79 ± 0.47	62.5 ± 19.4	49.8 ± 19.0	0.92 ± 0.91	15 – 40
26 April 2001 11:26:52 – 11:28:08	1.04 ± 1.42	74.4 ± 41.4	73.3 ± 36.9	2.99 ± 9.06	20 – 220
26 April 2001 11:28:28 – 11:29:19	0.63 ± 0.61	80.4 ± 31.8	71.2 ± 42.4	0.89 ± 1.68	40 – 300
26 April 2001 11:29:21 – 11:31:05	0.34 ± 0.32	89.8 ± 41.4	73.6 ± 37.4	0.37 ± 0.49	30 – 1300
26 April 2001 11:42:20 – 11:42:52	0.26 ± 0.20	98.3 ± 54.5	80.2 ± 44.7	0.30 ± 0.40	20 – 140
19 July 2001 10:04:16 – 10:05:15	0.32 ± 0.21	63.8 ± 14.0	56.6 ± 28.4	0.32 ± 0.26	35 – 250
19 July 2001 10:05:30 – 10:06:29	0.15 ± 0.08	74.7 ± 22.4	51.0 ± 26.1	0.13 ± 0.13	25 – 60
19 July 2001 10:35:07 – 10:36:07	0.14 ± 0.12	81.1 ± 25.3	58.3 ± 29.4	0.11 ± 0.12	80 – 3000
19 July 2001 10:38:49 – 10:38:59	0.11 ± 0.19	57.1 ± 17.0	32.5 ± 16.2	0.08 ± 0.13	70 – 270
16 September 2001 7:42:31 – 7:42:35	0.0	163.7 ± 18.8	0.0	0.0	25 – 45
17 September 2001 8:22:22 – 8:22:52	0.14 ± 0.13	34.2 ± 6.1	34.7 ± 17.9	0.20 ± 0.27	20 – 90
20 September 2001 14:38:42 – 14:38:58	0.29 ± 0.25	53.1 ± 19.6	33.6 ± 10.6	0.25 ± 0.30	30 – 220
9 October 2001 11:00:48 – 11:01:45	~ 0	226 ± 117	~ 0	~ 0	35 – 100
22 November 2001 9:50:37 – 9:50:37	1.00	330	400	1.26	27
7 April 2002 14:19:42 – 14:19:44	~ 0	94.5 ± 27.3	~ 0	~ 0	25 – 180
18 November 2003 8:35:00 – 8:36:00	0.39 ± 0.25	80.1 ± 15.2	91.3 ± 48.5	0.53 ± 0.57	210 – 1200
18 November 2003 8:36:12 – 8:37:48	0.24 ± 0.14	109.9 ± 27.2	115.0 ± 73.0	0.27 ± 0.22	50 – 550
18 November 2003 8:38:01 – 8:41:40	0.42 ± 0.28	77.6 ± 20.4	84.7 ± 49.9	0.52 ± 0.56	20 – 100
11 July 2005 16:34:22 – 16:36:17	0.26 ± 0.19	54.7 ± 18.8	43.1 ± 21.4	0.26 ± 0.29	50 – 2100

Table 3 (Continued.)

Event	I_a/I_e	d_e (ms)	d_a (ms)	$(I_a \cdot d_a)/$ $(I_e \cdot d_e)$	Intensity (sfu)
11 July 2005 16:36:22 – 16:36:59	0.09 ± 0.06	50.6 ± 13.6	37.2 ± 25.4	0.08 ± 0.09	50 – 300
11 July 2005 16:37:11 – 16:40:18	0.11 ± 0.11	70.9 ± 24.7	60.5 ± 29.3	0.11 ± 0.12	20 – 1000
15 April 2001 14:23:03 – 14:23:51	0.37 ± 0.35	68.8 ± 37.5	50.2 ± 27.0	0.38 ± 0.61	240 – 2650

3.6. 26 April 2001 Event at 1420 MHz, Interval 11:26:05 – 11:31:10 UT

In the range 1100 – 1600 MHz only fibers are present.

The first group of fibers was selected in the time interval 11:26:11 – 11:26:28 UT. The absorption is stronger than the emission in four cases.

The second group lasts longer and fibers are stronger. In two cases only absorption was present and in 12 cases the absorption was stronger than the emission, therefore the mean value of the parameters I_a/I_e and $(I_a \cdot d_a)/(I_e \cdot d_e)$ are stronger than in the previously considered intervals; their spread is also larger indicating very different characteristics for the studied fibers.

During the next enhancement (from 11:28:15 to 11:29:22 UT) many fibers show a complex structure; of the selected ones two show only emission and two only absorption.

In the following enhancement (11:29:20 – 11:31:10 UT) we selected about 100 fibers; 13 cases show only emission and three only absorption.

The mean value of the parameters I_a/I_e and $(I_a \cdot d_a)/(I_e \cdot d_e)$ are the highest for the first two groups (mainly during the second one) afterwards they are lower and lower. This trend lasts also in the interval that follows (after about ten minutes of no fiber presence).

3.7. 26 April 2001 Event at 1420 MHz, Interval 11:41:50 – 11:42:58 UT

This is the last (and lowest) enhancement of the continuum with fibers. They are present in the range 1000 – 1500 MHz and no other types of fine structures appear. For the selected fibers the part in absorption appears weaker than the one in emission and three events show only emission phase.

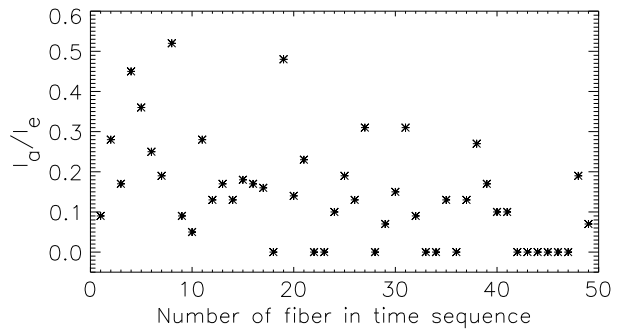
3.8. 19 July 2001 Event at 1420 MHz, Interval 10:01:50 – 10:06:35 UT

From 10:01:50 to 10:03:00 UT weak fibers are present in the range 1400 – 2000 MHz, but pulsations are stronger; so no fibers were selected for analysis.

The next enhancement (10:03:45 – 10:05:30 UT) contains a nice and representative group of fibers.

In the tail of the previous enhancement (10:05:30 – 10:06:35 UT) some weak fibers appear. The emission is always stronger than the absorption. The parameters I_a/I_e and $(I_a \cdot d_a)/(I_e \cdot d_e)$ show about half of the value pertinent to the previous quoted interval; however, the spread is very large. The spectrum shows that the continuum moves towards lower frequencies and becomes narrower (950 – 1500 MHz).

Figure 2 Ratio I_a/I_e for the fibers selected on 17 September 2001 (disposed in time sequence); start time 8:22:22 UT.



3.9. 19 July 2001 Event at 1420 MHz, Interval 10:27:35–10:29:05 UT

This complex enhancement is characterized by pulsations. Only afterwards, from 10:29:10 to 10:30:00 UT, some fibers are evident. As the activity is very complex (*i.e.* too many pulsations) it is difficult to find the fibers; we tentatively selected some of them but due to uncertainty they are not included in Tables 2 and 3.

3.10. 19 July 2001 Event at 1420 MHz, Interval 10:33:50–10:39:00 UT

In the last part of the strong enhancement (10:33:50–10:36:10 UT) we see some, generally strong, fibers. The continuum is present in the frequency range from < 800 to 1400 MHz. The part in emission is always stronger than the one in absorption and in nine cases the absorption phase is missing.

The enhancement from 10:36:10 to 10:39:00 UT is very strong. Pulsations, absorptions, and some fibers are evident only at frequencies > 1700 MHz.

During the last part of this enhancement (10:38:48–10:39:00 UT) some fibers (together with pulsations) that are evident in the spectrum were selected and studied. Their part in emission is prominent and the absorption phase is missing in about half of them.

3.11. 16 September 2001 Event at 1420 MHz, Interval 7:42:30–7:43:00 UT

The group of these fibers is very different from the other cases studied here: the continuum is very low. The fibers are few and appear in the spectrum between 1450 and 1100 MHz with low drift (typically -45 MHz s^{-1}), which shows irregular changes. No other fine structures are present. We selected only a few (complex) fibers; for this reason we considered the data after a weak smoothing. Absorption looks absent.

3.12. 17 September 2001 Event at 1420 MHz, Interval 8:22:00–8:23:00 UT

In the decaying part of the continuum dense fine structures appear superposed on a small enhancement. The selected fibers show weak absorption and 13 of them do not show this phase. In particular these are mostly present during the last part of the interval (among the last ten selected fibers six are absorption free). This is a nice example that shows the general tendency that the absorption phase is weaker for the “late” fibers. Figure 2 shows the trend of I_a/I_e for the selected bursts. The duration of these fibers is exceptionally short compared with the other considered cases. In the spectrum fibers appear in the frequency interval that is about 200 MHz wide and its central part moves from about 1200 MHz towards higher frequencies (up to about 1500 MHz).

3.13. 20 September 2001 Event at 1420 MHz, Interval 14:38:15–14:39:05 UT

The spectrum reveals the presence of pulsations and fibers in the range 900–2000 MHz, and we studied both of them in detail. Fibers, in general, appear later than pulsations, are stronger, and show longer duration. The part in emission of the selected fibers is always stronger than the one in absorption, and in four cases the absorption phase is missed.

3.14. 9 October 2001 Event at 1420 MHz, Interval 10:58:30–11:10:00 UT

Fibers appear in the range 1100–2000 MHz, their drift is positive (*i.e.* atypical) and high; different events show different values, typically it is about 220 MHz s^{-1} . The selected fibers appear without an absorption phase; they are long lasting due to their complex structure.

3.15. 22 November 2001 Event at 1420 MHz, Interval 9:50:10–9:50:42 UT

In the spectrum pulsations appear in the range 1100–2000 MHz. In the late part of the interval one fiber with evident absorption (range 1300–1500 MHz) appears. It was analyzed in detail, even if it is low and complex; the absorption phase is practically as strong as the emission one. Superposed on the decaying part of this fiber there is another one, still weaker and shorter; also in this case the absorption and emission parts are similar. In Tables 2 and 3 we report only the strongest and most prominent fiber.

3.16. 7 April 2002 Event at 1420 MHz, Interval 14:19:33–14:20:55 UT

The spectrum shows pulsations between 1000 and 2000 MHz; some fibers are present too but in a narrower interval (1200–1800 MHz). The fibers we were able to select are present in the early part of this interval (before 14:20:00 UT); it seems that the absorption phase is low or absent.

3.17. 18 November 2003 Event at 1420 MHz, Interval 8:33:40–8:41:40 UT

The spectrum shows pulsations between 1000 and 1800 MHz, some fibers are present too (range 1200–2000 MHz). After 8:36:00 UT the continuum is decaying and fibers are more evident and common than pulsations.

During the time when fibers are detected (8:35:00–8:41:40 UT) the emission phase is stronger than the absorption one; there are only two exceptions. This interval was divided in three parts (see Tables 2 and 3).

The mean value of the ratio I_a/I_e is higher in the first part than in the second one, in the third one it is the highest, however, also the spread is the largest.

3.18. 11 July 2005 Event at 1420 MHz, Interval 16:34:00–16:40:19 UT

In the spectrum the most evident fine structures are fibers, some of them are present in a very large frequency interval (1000–2000 MHz) and are very strong (up to instrumental saturation); some pulsations are present too, mainly from 16:34:35 to 16:34:55 UT and 16:37:00 to 16:37:28 UT.

The first group of the selected fibers (Tables 2 and 3) essentially contains the events recorded during the strongest enhancement. The emission phase is always stronger than the absorption phase and in two cases absorption is absent.

The second group of fibers is limited to the decaying part of the strongest enhancement; frequency range 1100–1500 MHz. The emission phase is predominant in respect to the absorption one and in two cases the absorption is not present.

In the interval 16:37:00–16:37:06 UT that contains pulsations and fibers we tried to select separately some events that belong (very probably) to the first and the second type of fine structures in order to find if it is possible to differentiate them according to their duration (as the polarization, as usual, is the same for both). We realized that the mean duration is (62.9 ± 7.6) ms and (56.0 ± 8.0) ms, respectively; so, in this case (but also in many other cases), it is not possible to discriminate between the two types of fine structures on the basis of their duration.

After 16:37:11 and up to 16:40:19 UT there are some sporadic enhancements and in the spectrum fibers are evident. The emission phase is always stronger than the absorption one and in six cases the absorption is missing (mainly in the last part of the interval).

The mean ratio I_a/I_e is stronger for the fibers present during the strongest enhancement and it is often zero in the late part of the presence of fibers. That confirms the tendency that this ratio is decaying with time.

4. Fitting of a Typical Fiber-Burst Profile

For fitting of a typical fiber-burst profile, we interpret the observed fibers as the result of a modulation of the continuum radio emission by density pulses or waves of the fast sausage magnetoacoustic type (Karlický, Mészárosová, and Jelínek, 2013). Note that similar model was proposed to explain some zebra structures (Karlický, 2013).

In modeling of the fibers, in agreement with Kuznetsov (2006), we assume that the radio emission is produced at the double (harmonic) upper-hybrid frequency as a result of a coalescence of two upper-hybrid waves, generated by the loss-cone instability of superthermal electrons. Furthermore, we assume that the radio emission is generated uniformly in the whole interval of the considered source heights. The intensity of the radio emission at some specific frequency thus depends only on the gradients of the electron density and magnetic field intensity, n_e and B , in the radio source, *i.e.* the wave perturbation modulates the frequency dependence of the radio emission.

We use the Aschwanden (2002) density model of the solar atmosphere. For simplification and owing to low values of the electron-cyclotron frequency in comparison with the electron-plasma frequency in coronal conditions, we neglect the role of the magnetic field in this fitting. Thus, the maxima of fibers are produced at the locations with minimum density gradients and the emission depressions correspond to the maximum density gradients. The resulting radio flux at a specific frequency f can be expressed as the sum of emissions from plasma volumes having the upper-hybrid frequency f_{up} close to $f/2$.

In the present analysis we use two methods:

- i) Fitting of the observed fibers by modeled ones.
- ii) Direct derivation of the pulse density profile based on observed fiber data.

4.1. Method 1: Fitting of the Observed Fiber

In this method, we assume the density perturbation to be

$$n_e^{\text{pert}}(h) = n_0^{\text{pert}} \exp \left[- \left(\frac{h - h_0}{d_s} \right)^2 \right], \quad (1)$$

Figure 3 Example of the 1420 MHz L-polarized (continuous line) and R-polarized (dashed line) radio-flux profiles of the fiber burst observed from 14:38:52.3 to 14:38:52.6 UT on 20 September 2001.

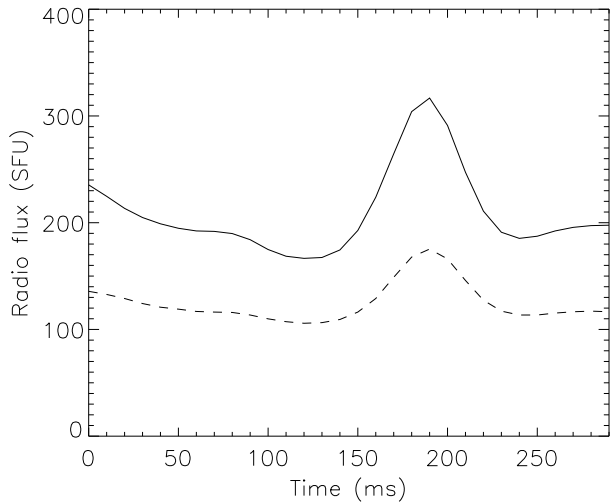
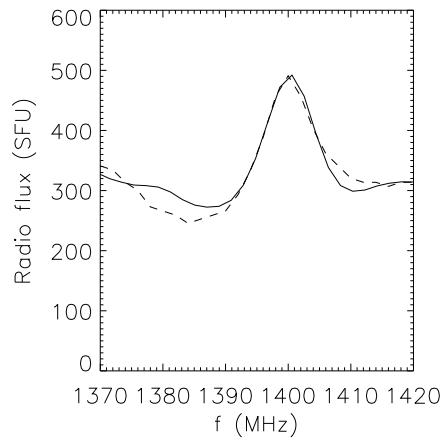


Figure 4 Frequency profile of the fiber burst transformed from that in Figure 3 (R+L polarization) (continuous line). The fitted profile is shown by dashed line.

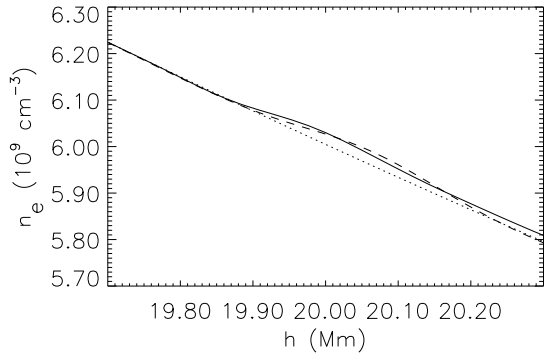


where n_0^{pert} is the perturbation amplitude, h is the height in the atmosphere, h_0 is the position of the perturbation, and d_s is the spatial width of the perturbation. This density perturbation is then superimposed on the density profile of the solar atmosphere.

In our case we measure the fiber-burst profiles at a single frequency with high time resolution (up to 0.01 s); see the example in Figure 3. As the frequency resolution of fibers is generally very low, we measure from the corresponding radio spectrum the frequency drift (in the 20 September event it is -194 MHz s^{-1}) and we transform the time-flux fiber profile into frequency-flux profile (R+L); see the continuous line in Figure 4.

Changing n_0^{pert} , d_s , and h_0 we can generate density pulses of different forms. For each combination of parameters we compute the modeled frequency profiles of fibers, which we compare with that observed. The best fit of the frequency fiber profile is shown by the dashed line in Figure 4. This fit is obtained for the perturbation parameters as follows: $n_0^{pert}/n_e(h_0) = 0.005$, $d_s = 180 \text{ km}$, and $h_0 = 20.06 \text{ Mm}$. This density pulse, superimposed on Aschwanden's (2002) density model, is shown by the dashed line in Figure 5.

Figure 5 Density n_e vs. height h according to Aschwanden's (2002) density model of the solar atmosphere (dotted line). The dashed and continuous lines correspond to the density profiles derived by the method 1 and 2, respectively, obtained by fitting the 20 September 2001 fiber.



4.2. Method 2: Direct Derivation of the Pulse Density Profile

Using method 1 the question arises if the density perturbation profiles could be derived directly from the frequency fiber profile shown by the continuous line in Figure 4. Therefore, we make the following computations. We assume that the basic gradient in the atmosphere (which corresponds to the background-continuum level of radio flux) is the one in Aschwanden's (2002) density model, *i.e.*

$$\frac{dn_e}{dh} = -p \frac{n_e(h)}{h}, \tag{2}$$

where p is the model constant $p = 2.38$. Then the gradient modified by the perturbation can be expressed as

$$\frac{dn_e}{dh} = -p \frac{n_e(h)}{h} \frac{I_0}{I}, \tag{3}$$

where I is the radio flux at different frequencies along the fiber-burst profile and I_0 is the reference radio flux corresponding to the background-continuum radio flux.

Calculating these gradients at all fiber frequencies and starting from the highest frequency of the fiber profile (*i.e.* from the highest density) we can step by step integrate the density profile. The result is shown by the continuous line in Figure 5. As can be seen, the density profiles derived by both methods are similar.

5. Discussion and Conclusions

Looking in the archives of solar radio data at the Trieste Astronomical Observatory (radio-polarimetric observations at 1420 and 2695 MHz) and at the Astronomical Institute in Ondřejov (spectra in the ranges 800–2000 and 2000–4500 MHz) we found 18 radio events that contain fibers (on 13 days). We divided them into 26 groups (generally at 1420 MHz and one at 2695 MHz) and we selected about 700 fibers for detailed study. These groups present their own peculiarities, both in the single frequency plots and in the spectral data. Our main interest was the study of these very different characteristics that can be obtained from high time resolution single frequency records when also circular polarization characteristics are at disposal. Contemporaneous spectral data ensure us that the studied bursts are fibers.

We realized that fibers can appear during strong and long lasting flares, generally they are present in the late phase of the flare, however, they appear also near the maximum or even in the growing phase of the associated flare. Fibers are generally superposed on rather strong continua. The polarization of fibers is practically the same as the polarization of the associated continuum. We found polarization degrees from about 0 to extremely high values.

In a group of fibers their drift (generally negative) is not homogeneous; rough limits are $-45 - (-110)$ MHz s⁻¹ at 1420 MHz; for the group at 2695 MHz it is roughly -300 MHz s⁻¹. For one group we found a positive drift.

For each selected fiber we evaluated (in sfu) its emission I_e (above the continuum) and absorption I_a (below the continuum). However, the trend of the continuum is not easy to trace. Another related problem deals with the measurement of the (generally weaker) duration of the absorption d_a , as it can be disturbed by weak bursts (and/or noise) that are very common in the continuum. The duration of the emission phase d_e is determined with greater confidence. The spread of the d_e mean values is very large (from 34 to 330 ms) and the one of d_a is similar. However, it is certain that the ratio I_a/I_e and also the values $(I_a \cdot d_a)/(I_e \cdot d_e)$ are very different even for nearby fibers. In a group of fibers the mean values of I_a/I_e and $(I_a \cdot d_a)/(I_e \cdot d_e)$ are similar, however, the spread is large (of the order as the mean value itself) and still larger for $(I_a \cdot d_a)/(I_e \cdot d_e)$. We found that eight groups show low mean ratio I_a/I_e (< 0.20), in two cases it is equal to zero, but these two groups are formed by a low number of selected events; four groups present rather strong values (> 0.60) and in one case only one fiber is considered; the majority of mean values are in the range $0.24 - 0.42$. We studied in detail a great number of selected fibers in order to find the different characteristics that can be present in such phenomena. In particular we realized the tendency that “late” fibers in a group show lower ratio of I_a/I_e (and $(I_a \cdot d_a)/(I_e \cdot d_e)$). The ratio of I_a/I_e (and $(I_a \cdot d_a)/(I_e \cdot d_e)$) for the 2695 MHz fibers is comparable to the ones at 1420 MHz.

It is not rare to see broadband pulsations almost simultaneously with fibers (in 55 % of cases). We also measured the duration of about 300 selected pulsations. The range of the mean duration of pulsations being rather limited (40–64 ms) it is sometimes possible (*i.e.* when fibers are “long” lasting) to discriminate between the two types of “fine structures” according to their duration. The polarization of pulsations is practically the same as for the contemporaneous fibers and the underlying continuum. When a delay between the polarimetric channels is present, it is the same for fibers and pulsations.

Using the recent model by Karlický, Mészárosová, and Jelínek (2013) we successfully fitted a typical fiber burst recorded at 1420 MHz on 20 September 2001. Moreover, we derived the density pulse profile generating the fiber burst directly from its frequency profile. This shows that this simple model can explain some aspects of fiber bursts. This model is supported by the similarity of parameters related to fibers and frequently associated pulsations. While pulsations are commonly explained by magnetohydrodynamic oscillations of loops, the fibers in the present interpretation are generated by propagating fast sausage magnetohydrodynamic pulses or waves. The present model of fibers can be further improved considering that the modulation of the radio emission by waves is not only due to the variation of the density gradient, but also by modulation of the radio emission itself, *e.g.*, through wave changes of the magnetic field, and thus changes of the growth rate of the loss-cone instability. The trend showing the decrease of I_a/I_e in some groups of fibers with time remains unclear. We can only speculate that there may be an increasing number of weak fibers and/or increasing radio-flux noise implies a decrease of I_a with time.

Recently an article regarding fibers at 327 MHz (recorded on 17 April 2002 from 9:42:51 to 9:44:11 UT) was published by Berhondo *et al.* (2013). This article is devoted to the analysis of the deterministic behavior of such an activity, however, in the article and from other

detailed measurements we find some similarities and differences in respect to the results at higher frequencies here reported. At 327 MHz the continuum appears to be more easily determined. The ratio I_a/I_e is still very different even for nearby fibers. The number of cases with absorption stronger than emission is practically the same but opposite (*i.e.* the mean ratio I_a/I_e is about one), and this looks like the main difference when comparing the characteristics of fibers at 327 MHz and at higher frequencies here considered. The mean duration of d_e is 406 ms. As the duration of plasma emission phenomena is changing according to the inverse of the frequency, this value should correspond to 93 ms at 1420 MHz. The mean duration of d_a is 371 ms; this value should correspond to 85 ms at 1420 MHz. These mean values of d_e and d_a derived on the basis of the characteristics of fibers at 327 MHz, are not far from the ones reported in this paper.

We used the model of Karlický, Mészárosová, and Jelínek (2013) mainly due to its simplicity, which enables us to make the inverse procedure, *i.e.* to compute the density wave profile from the fiber-burst profile. The model can consider a wave train for a series of fibers and also an individual wave pulse for an individual fiber, as in the present paper. If these pulses are generated randomly in time then the fibers are distributed randomly, too. Even in the case of a wave train the fibers need not be strictly periodic because the wave train in some of its parts is not periodic. As shown by Roberts, Edwin, and Benz (1984) the sausage wave train has three phases: a small amplitude periodic phase, a strong amplitude quasi-periodic phase, and a decay phase. Furthermore, this wave train propagates in a gravitationally stratified atmosphere, which for a finite-amplitude wave train also leads to deviations from strict periodicity. This might explain the low-dimensional deterministic process found for the 327 MHz fibers by Berhondo *et al.* (2013).

In the fitting procedure we neglected the magnetic field intensity as in coronal conditions the electron-cyclotron frequency is lower than the electron-plasma frequency. However, the magnetic field intensity remains important for the fiber-burst polarization. The emission with the high polarization degree is more probable at the fundamental (upper-hybrid) frequency than at its harmonic. The same fitting procedure as presented here can be made also for the fundamental (upper-hybrid) frequency. The derived densities will be different, but this computation does not give principally new results. The reason why we considered here the emission at the harmonic frequency is that for a high-density bump, some emission from behind this bump need not escape and it would complicate the computations. Because we observed the fibers with the polarization degrees from about zero to high values, it looks like that some fibers were generated at harmonic and some at fundamental frequencies.

Acknowledgements The authors thank the referee (Dr. G.P. Chernov) for comments that improved the paper. This research was supported by the grant P209/12/0103 (GA CR), the project RVO:67985815 of the Astronomical Institute of the Academy of Sciences of the Czech Republic, and the Marie Curie PIRSES-GA-2011-295272 RadioSun project. The authors acknowledge Mr. S. Padovan and Mr. I. Coretti (INAF – Trieste Astronomical Observatory) for their care in instrument maintenance and radio data recording. The program for radio data calibration and reduction was prepared by Mr. S. Padovan.

References

- Aschwanden, M.J.: 2002, *Space Sci. Rev.* **101**, 188.
 Benz, A.O., Mann, G.: 1998, *Astron. Astrophys.* **333**, 1034.
 Berhondo, A.L.M., Rodriguez, A.K.D., Zlobec, P., Perez, L.C.: 2013, *Astrophys. Space Sci.* **346**, 301.
 Bernold, T.E.X., Treumann, R.: 1983, *Astrophys. J.* **264**, 677.
 Chernov, G.: 1976, *Soviet Astron.* **20**, 449.
 Chernov, G.: 2011, *Fine Structure of Solar Radio Bursts*, Springer, Berlin.
 Chernov, G.P., Zlobec, P.: 1995, *Solar Phys.* **160**, 79.

- Elgaroy, O.: 1982, *Report of the Institute of Theoretical Astrophysics* **53**, Blindern.
- Fleishman, G.D., Fu, Q.J., Huang, G.-L., Melnikov, V.F., Wang, M.: 2002, *Astron. Astrophys.* **385**, 671.
- Jiřička, K., Karlický, M., Kepka, O., Tlamicha, A.: 1993, *Solar Phys.* **147**, 203.
- Karlický, M., Mészárosová, H., Jelínek, P.: 2013, *Astron. Astrophys.* **550**, A1.
- Karlický, M.: 2013, *Astron. Astrophys.* **552**, A90.
- Kuijpers, J.: 1975, *Solar Phys.* **44**, 143.
- Kuznetsov, A.A.: 2006, *Solar Phys.* **237**, 153.
- Mann, G.: 1990, *Astron. Nachr.* **311**, 409.
- Mann, G., Karlický, M., Motschmann, U.: 1987, *Solar Phys.* **110**, 381.
- Rausche, G., Aurass, H., Mann, G., Karlický, M., Vocks, C.: 2007, *Solar Phys.* **245**, 327.
- Roberts, B., Edwin, P.M., Benz, A.O.: 1984, *Astrophys. J.* **279**, 865.
- Slotje, C.: 1981, Atlas of fine structures of dynamic spectra of solar type IV-dm and some type II radio bursts. Dwingeloo.
- Treumann, R.A., Güdel, M., Benz, A.O.: 1990, *Astron. Astrophys.* **236**, 242.
- Wang, S., Zhong, X.: 2006, *Solar Phys.* **236**, 155.
- Young, C.W., Spencer, C.L., Moreton, G.E., Roberts, J.A.: 1961, *Astrophys. J.* **133**, 243.
- Zlobec, P., Karlický, M.: 1998, *Solar Phys.* **182**, 477.